

A Rolling Shutter Compliant Method for Localisation and Reconstruction

Gaspard Duchamp, Omar Ait-Aider, Eric Royer and Jean-Marc Lavest

Institut Pascal - COMSEE, Universite Blaise Pascal, Clermont-Ferrand, France

Keywords: Rolling Shutter, Reconstruction.

Abstract: Nowadays Rolling shutter CMOS cameras are embedded on a lot of devices. This type of cameras does not have its retina exposed simultaneously but line by line. The resulting distortions affect structure from motion methods developed for global shutter, like CCD cameras. The bundle adjustment method presented in this paper deals with rolling shutter cameras. We use a projection model which considers pose and velocity and need 6 more parameters for one view in comparison to the global shutter model. We propose a simplified model which only considers distortions due to rotational speed. We compare it to the global shutter model and the full rolling shutter one. The model does not need any condition on the inter-frame motion so it can be applied to fully independent views, even with global shutter images equivalent to a null velocity. Results with both synthetic and real images shows that the simplified model can be considered as a good compromise between a correct geometrical modelling of rolling shutter effects and the reduction of the number of extra parameters. Keywords

1 INTRODUCTION

CMOS sensors are more and more used for embedded systems due to its low power consumption, low price, and high sensitivity. Basics CMOS sensors acquire image row by row, this mode allows a lighter and faster electronic system giving a better frame rate. The drawback is a deformation of the image due to the relative motion camera/scene. This distortion can be a problem when trying to catch the motion or to reconstruct the environment when embedded on a mobile system (Royer et al., 2007). The rise of 3D reconstruction in urban context using cameras embedded on cars and photos collection got from the web are dependent on the capability of the system to deal with such acquisitions. Different way to correct distortion introduced by the rolling shutter or to take advantage from them in the literature. One way is to undistort the entire image (Liang et al., 2008), (Baker et al., 2010), (Bradley et al., 2009). This kind of methods gives correct visual results but is not satisfying because it does not deal with 3D structure of the scene. (Ait-Aider et al., 2006) and (Ait-Aider et al., 2007) solved the PNP problem of a moving object of known geometry by taking advantage of image distortion to get the speed of the target simultaneously with the pose. (Meingast et al., 2005) gives a method to get

a temporal calibration of the rolling shutter, and a correct model for small rotational speed and fronto-parallel motion. (Magerand et al., 2012) propose a polynomial projection model and a constrained global optimization technique in order to solve the minimal PNP problem without any initial guess of the solution making the method more suitable for automatic 3D-2D matching in a RANSAC framework. (Meiland et al., 2013) proposes a unifying model for both motion blur and rolling shutter distortions for dense registration. Recently, few works adressed the problem of structure from motion using rolling shutter image sequences. (Ait-Aider and Berry, 2009) studied 3D reconstruction and egomotion recovering using a calibrated stereo rig. (Hedborg et al., 2012) presents a bundle adjustment method which computes structure and motion from a rolling shutter video exploiting the continuity of the motion across a video sequence. (Saurer et al., 2013) consider the stereo in the case of a fast moving vehicle where rotational speed is neglected and where Rolling Shutter effects are supposed to be affected principally by the depth of the scene. A recent way to handle reconstruction is not to consider discrete poses of a camera along a trajectory, but a continuous time motion in space as do (Anderson and Barfoot, 2013). Finally, (Li et al., 2013) proposes an approach to correct the reconstruction using

inertial sensors which are more and more embedded on devices like smartphones or notepads.

1.1 Related Work and Contribution

The closest work to ours, is the one presented in (Hedborg et al., 2012). Rolling shutter bundle adjustment is achieved by exploiting the continuity of the motion across a video sequence. A key rotation and translation is associated to the first row of each frame as in classical bundle adjustment. In addition, the poses attached to the rest of image rows are interpolated from each pair of successive key pose parameters using SLERP interpolation. The basic idea is to assume that the trajectory and pose variation between frames are smooth. The advantage of this approach is that only six extra parameters are used for the entire sequence in comparison to classical bundle adjustment. Nevertheless, it seems evident that the inter-frame motion should be very small to ensure that interpolated rotations and translation fit the actual values. As result, the approach requires a high frame rate as in the experiments presented in the paper. This increases the risk of data bottleneck and/or limits the dynamic performances in real time applications such as SLAM with mobile robots. In addition, the quality of motion estimation and triangulation is always better when the inter-frame motion is significant. Therefore, it seems to us that a method which estimates independent cameras without any assumption about motion parameters during inter-frame intervals is more pertinent. In the work presented in (Saurer et al., 2013) the authors presented a dense multi-view stereo algorithms that solve for time of exposure and depth, even in the presence of lens distortion. The camera is supposed to be embedded on vehicle and rotational speed is neglected so that Rolling Shutter effects are supposed to be affected principally by the depth of the scene. Unfortunately, as it stated in (Meilland et al., 2013) and (Ringaby and Forssén, 2012), in practice the lateral rotational movements are the most significant image deformation components, a simulation of the optical flow is done in the paper to confirm the effect of rotations and translations on rolling shutter distortion. In this paper we present a bundle adjustment method to be used with rolling shutter cameras basing on the work of (Ait-Aider et al., 2006). The approach can be applied to totally independent views since no assumption is done on the type of motion between the cameras. The speed parameters concerns only the motion during the very short time of each frame scan-line exposure. Particularly we analyze the effect of each type of motion and propose a simplified model which considers rolling shutter effects due to rotational speed

only. We make an analyse of the optical flow according to the speed, and justify the Omission of linear speed. This comes from the assumption that rotation produces more significant optical flow and thus bigger image distortions. We make a comparative study of 3 projection models: the classical Global Shutter, the complete rolling shutter model with both rotational and linear speed and the simplified rolling shutter model. Results with both synthetic and real images shows that the simplified can be considered as a good compromise between a correct geometrical modelling of rolling shutter effects and the reduction of the number of extra parameters.



a



b

Figure 1: Illustration of a rolling shutter effect: still camera, equivalent to global shutter (a), moving rolling shutter camera (b).

2 PROJECTION MODELS

2.1 Global Shutter

Considering the classical pinhole camera model defined by its intrinsic parameters Tsai (Tsai, 1986), the projection equation of a 3D point $P = [X, Y, Z]^T$, with

$[R T]$ the transformation between the object and the camera frame is (Hartley and Zisserman, 2003):

$$s\tilde{\mathbf{m}} = \mathbf{K}[\mathbf{R} - \mathbf{R}\mathbf{T}]\tilde{\mathbf{P}} \quad (1)$$

where s is an arbitrary scale factor, \mathbf{K} the matrix the intrinsic parameters of the camera, $\mathbf{m} = [u, v]^T$ the perspective projection of \mathbf{P} noting $\tilde{\mathbf{m}}$, $\tilde{\mathbf{P}}$ the homogeneous coordinates of \mathbf{m}, \mathbf{P} .

2.2 Rolling Shutter

The projection equation of this point considering a uniform motion during the time of one image scanning with a rolling shutter camera is:

$$s\tilde{\mathbf{m}}_i = \mathbf{K}[\delta\mathbf{R}_i\mathbf{R} - \delta\mathbf{R}_i\mathbf{R}(\mathbf{T} + \delta\mathbf{T}_i)]\tilde{\mathbf{P}}_i \quad (2)$$

where τ is the delay from a line to the next one, $\delta\mathbf{R}_i$ is the amount of rotation due to rotational velocity at the time corresponding to the line $\tau \cdot v_i$, and $\delta\mathbf{T}_i$ the amount of translation due to translational velocity at this time. The index i is for the i^{th} 3D point, v_i its corresponding line on the sensor and $t_i = \tau \cdot v_i$ the delay in acquisition from the first line to the line of the current 3D point i .

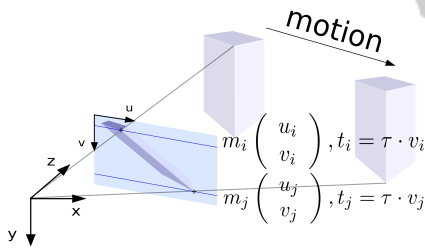


Figure 2: Perspective projection of a moving object with a rolling shutter camera.

2.3 Simplified Rolling Shutter

Removing the linear speed from the Rolling shutter model gives us the following projection equation:

$$s\tilde{\mathbf{m}}_i = \mathbf{K}[\delta\mathbf{R}_i\mathbf{R} - \delta\mathbf{R}_i\mathbf{R}\mathbf{T}]\tilde{\mathbf{P}}_i \quad (3)$$

2.3.1 Optical Flow from Speed

The third model tested here is made with the assumption that the rolling shutter effect due to translation is negligible compared to the one due to rotation. The effect induced by a linear motion parallel to the retina is slightly the same as a rotational motion of the camera according to an axe perpendicular to the linear displacement. In the case of a frontal motion (camera placed at the front or the rear of a vehicle), no rotational motion can have the same effect and the model with only rotational speed cannot compensate,

but in this case the optical flow consecutive to the linear motion is reduced. Fig. 3 shows the optical flow induced by the motion of the camera. Translations have a very lower effect and become quickly indistinguishable with depth of the view.

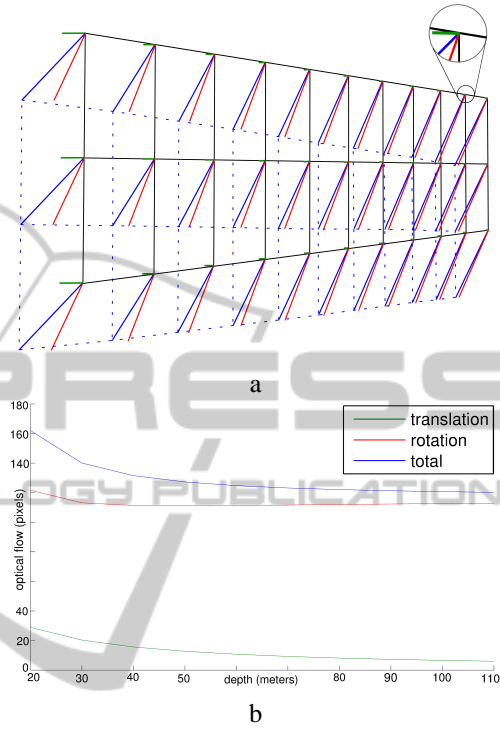


Figure 3: Simulated image of an object and the optical flow inherent to the camera motions, green: translation (10 m/s), red : rotation (2 rad/s), blue : both (a), optical flow expressed in pixels according to depth of the scene for each type of motion.

3 3D RECONSTRUCTION WITH ROLLING SHUTTER

We consider several views of a scene, each taken from a moving rolling shutter camera. We want to get the pose of each cam of each view and the position of 3D points from 2D-2D detection correspondence. Previous work (Hedborg et al., 2011) considers one pose for each line of the image, here we consider a unique pose for each view, and the distortion is compensated by a small motion depending of the speed and the retina line (proportional to time since the beginning of the acquisition). By expressing the entire system in a single camera coordinate we get:

$$s\tilde{\mathbf{m}}_i = \mathbf{K}[\delta\mathbf{R}_{i\text{left}} - \delta\mathbf{R}_{i\text{left}}\delta\mathbf{T}_{i\text{left}}]\tilde{\mathbf{P}}_i \quad (4)$$

the projection equation in the camera chosen for being the reference.

$$\tilde{\mathbf{s}}_i = \mathbf{K}[\mathbf{R}\delta\mathbf{R}_{\text{iright}} - \mathbf{R}\delta\mathbf{R}_{\text{iright}}(\mathbf{R}\delta\mathbf{T}_{\text{iright}} + \mathbf{T})]\tilde{\mathbf{P}}_i \quad (5)$$

the projection equation for the other cameras.

We get $2N$ reprojection equations for each 3D point (two in each image), each 3D point has 3 parameters and we have twelve parameters for each additional camera pose. Thus, we need at least eighteen points plus twelve per pose to solve the problem against six plus six for the global shutter model. In case of the simplified rolling shutter model, we only need at least twelve points plus nine per pose.

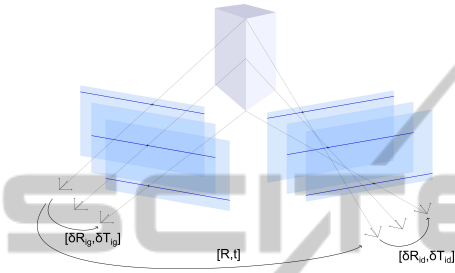


Figure 4: Two different views of a scene taken by moving rolling shutter cameras.

This leads us to minimize the following cost function with respect to pose $(\mathbf{R}_j, \mathbf{T}_j)$ (first camera is at world reference), rotational speed (\mathbf{W}_j) and translational speed (\mathbf{V}_j) parameters of j^{th} view:

$$\varepsilon(\mathbf{R}, \mathbf{T}, \mathbf{W}, \mathbf{V}) = \sum_{j=1}^k \sum_{i=1}^l [\mathbf{m}_{ij} - \mathbf{p}_{ij}]^2 \quad (6)$$

\mathbf{p}_{ij} being the detected points in j^{th} image and \mathbf{m}_{ij} , the projection in j^{th} image of the 3D point \mathbf{P}_i associated to \mathbf{p}_i and \mathbf{q}_i .

An initial solution can be found using the epipolar constraint. It can be more precise by adding a step after initialization; we must consider an essential matrix per point pair instead of per image pair fig. 4.

$$\mathbf{q}_i^T \mathbf{E}_i \mathbf{p}_i = 0 \quad (7)$$

With:

$$\mathbf{E}_i = \hat{\mathbf{T}}_i \mathbf{R}_i \quad (8)$$

$\hat{\mathbf{T}}_i$ is the antisymmetric matrix associate to \mathbf{T}_i and:

$$\mathbf{R}_i = \delta\mathbf{R}_{\text{left}}^T \mathbf{R} \delta\mathbf{R}_{\text{right}} \quad (9)$$

$$\mathbf{T}_i = \delta\mathbf{R}_{\text{left}}^T (\mathbf{R} \delta\mathbf{T}_{\text{right}} + \mathbf{T} - \delta\mathbf{T}_{\text{left}}) \quad (10)$$

This leads us to a non linear system, whereas it is, for global shutter images. In this step the linear speed is ignored. The 3D structure is obtained by triangulation.

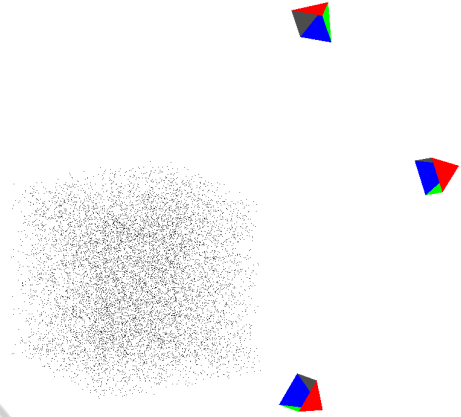


Figure 5: Schematic view of the experimental setup with synthetic data.

4 EXPERIMENTS

4.1 Test with Synthetic Data

4.1.1 Experimental Setup

To test the reconstruction, a first stage was to use synthetic data. An object was created as a 3D point cloud. Cameras with their own speed and pose were placed around watching towards it. there is no correlation between the orientation of the speed and the displacement between each view. Each image of the scene is considered as totally independent. Images were obtained by application of the rolling shutter projection equation. Resolution of the problem was then done for each model, global shutter, rolling shutter and simplified rolling shutter. The virtual object was included in a cube of 25m edge placed at 75m to 125m from the cameras.

Simulated cameras resolution was 1600 per 1200 pixels, the focal was 6.5mm, τ was set to $25\mu\text{s}$. Cameras speed magnitude was in range $[0, 10]m/s$ and $[0, 2]rad/s$ for linear and angular speed. Those parameters were chosen to keep the object in the vision field and the speeds according to the ones available for a pedestrian or the autonomous vehicle VIPA (<http://www.ligier.fr/ligier-vipa>). A noise on measures was applied in range $[0, 1]pixel$, the number of 3D points in range $[200, 1000]points$ and the number of views in range $[2, 10]images$. All of those parameters are shown in the table 1. For each set, 100 simulation were done and solved with each model. The number of simulations is 2673000.

Fig. 6 and 7 show the loss of accuracy of the three models according to speed.

Table 1: List of parameters used for the simulation.

	views	3d pts	angular speed	linear speed	noise
Min	2	200	0	0	0
Max	10	1000	2	10	1
Step	1	200	0.25	2	0.1
Steps	9	5	9	6	11

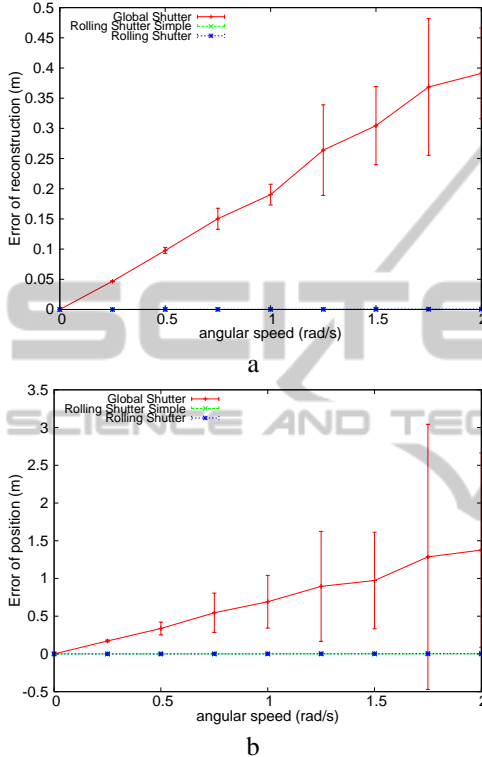


Figure 6: Errors of reconstruction (a), position of cameras (b) according to rotational speed.

4.1.2 Noise

In this section we study robustness of the model to noise. We added a random geometric noise following a uniform distribution from 0 to 1 pixel every 0.1 pixel. Each measure is a mean of 100 simulations following the same scheme as previously for a speed corresponding to $[10m/s, 2rad/s]$. As one can see on fig. 8, the addition of degrees of freedom to the system makes it less robust to noise. It needs more views of the scene and more 3D points to get the system constrained enough and the reconstruction robust to a high noise level when using the complete rolling shutter model. The simplified rolling shutter model is more robust. Fig. 9 (a) shows the precision of reconstruction according to the number of cameras for a speed and noise corresponding to $[10m/s, 2rad/s, 0.5pixel]$ and 600 3D points, and (b)

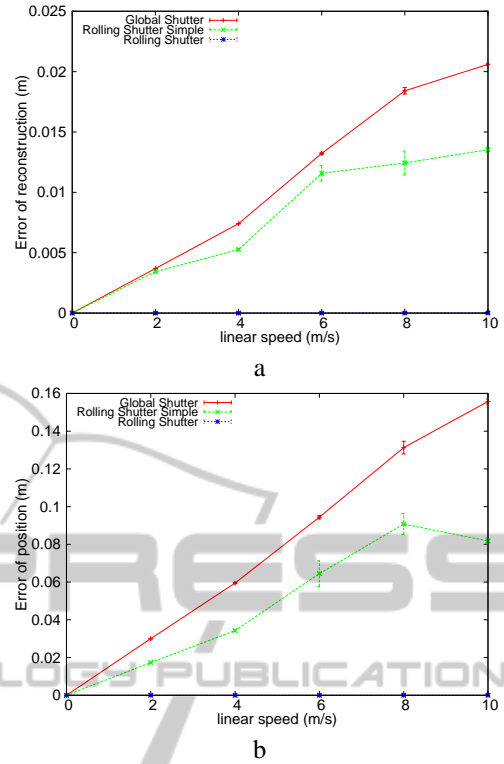


Figure 7: Errors of reconstruction (a), position of cameras (b) according to translational speed.

the precision of reconstruction according to the number of 3D points for a speed and noise corresponding to $[10m/s, 2rad/s, 0.5pixel]$ and 4 views.

4.2 Experiment with Real Data

4.2.1 Sensor Calibration of Parameter Tau

Objective removed, all the cells of the sensor are exposed at the same time to a flashing light whose frequency is known. The frequency of the light is high enough regarding the rolling shutter frequency to see several flashes. The lag between each line of the sensor is deduced by a simple ratio between periods of the light signal and the number of lines it overlaps. The time found for our camera is $110\mu s$.

4.2.2 Reconstruction

To illustrate the relative robustness of the simplified rolling shutter model beside the complete one, and the gain of precision from the global shutter one, it was tested to reconstruct a 3D structure. The chosen structure is a corner to easily visually check if any deformations occurs during the reconstruction. We can see on Fig. 11 that the reconstruction presents no apparent distortions on the global structure, this is more

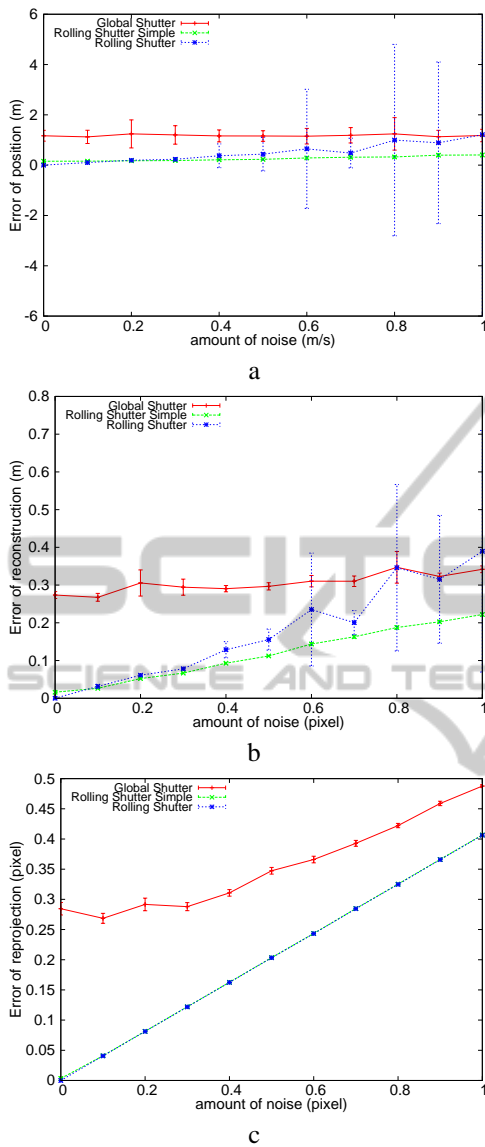


Figure 8: Errors of position of cameras (a), reconstruction (b), reprojection (c) according to noise, with randomly oriented speeds of $2rad/s$.

evident to see on the attached video. The camera used is a webcam logitech C310, used with a resolution of 640 by 480 pixels and a focal distance of 4 mm. The final parameters of reconstruction such as the number of inlier 3D points, inlier observations, and final reprojection error RMS are shown in table 2.

Table 2: Results of the reconstruction.

	3dpts	observation	rms
Global Shutter	2537	10615	0.86
Rolling Shutter	3273	13204	0.84
Rolling Shutter Simple	3446	13639	0.77

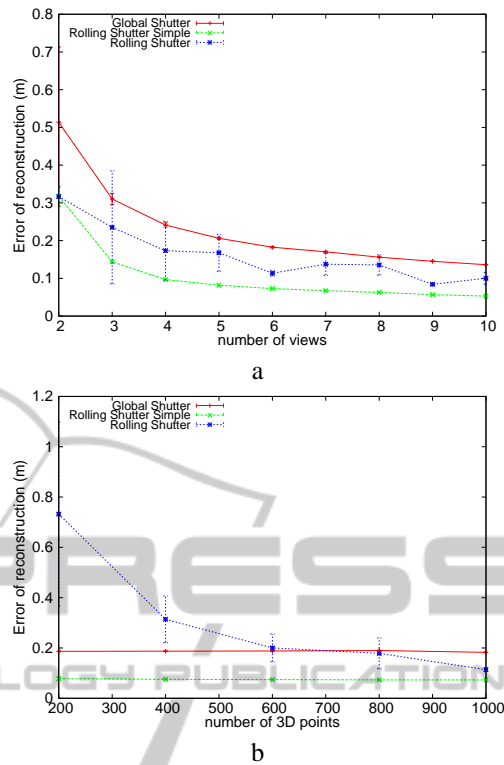


Figure 9: Errors of reconstruction according to the number of views (a), to the number of 3D points (b).

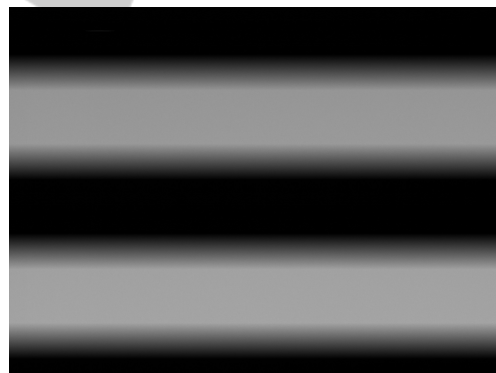


Figure 10: Image used for the temporal calibration of CMOS rolling shutter sensor. Objective removed, all the cells of the sensor are exposed at the same time to a flashing LED whose frequency is controlled with a square signal generator and an oscilloscope (Meingast et al., 2005).

5 DISCUSSION

In addition to the presentation of the simplified rolling shutter model, the results in Fig.6 and 7 show that the impact from linear speed on the quality of the reconstruction is less than the one from the rotational speed in the same way of the optical flow previously studied. As well the addition of variables to the system

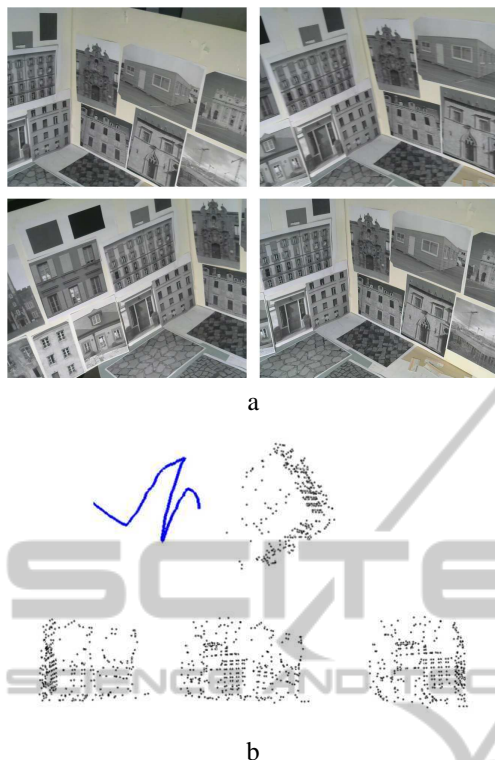


Figure 11: Motion and reconstruction of a trajectory, (a) some images used for the reconstruction, (b) in blue the motion of the camera and in black the 3D reconstruction from different point of view.

makes it less constrained and so cause a decay in its robustness to noise. According to Fig. 8 and 9 the simplified rolling shutter model is more robust than the complete one. In addition, it is faster to solve (less parameters to optimise, less derivation a fortiori numerical ones, smaller jacobians). Less variables reduces too the probability to have local minima.

A system which doesn't need successive sequences of near images allow to work with spatially and time spaced images (leading better triangulation due to a more pronounced stereo), the inclusion of images taken out of the sequence both rolling and global shutter. It results a lighter application with less processor charge and less data transfer via the bus. Currently the methods in reconstruction are not in using all the images from the camera but selecting them, as seen in (Mouragnon et al., 2009). The presented method is suitable in the actual state of art SLAM by its spatially and temporally spaced acquisition robustness.

6 CONCLUSIONS

We presented a method to deal with rolling shutter distortion for SFM applications relevant in the current state of art. The method is accurate thanks to the modelling of the motion; generic, it can deal with both rolling shutter and global shutter images; robust thanks to the use of only very useful parameters; usable with very low frame rate video. We think that this method can be very useful in many applications in robotics, or in augmented reality applications with the use of devices such as phones or notepads whose embedded cameras are rolling shutter. We envisage to use the effect of rolling shutter on primitives to get a priori on motion and robustify matching.

ACKNOWLEDGEMENT

This work has been sponsored by the French government research program Investissements d'avenir through the RobotEx Equipment of Excellence (ANR-10-EQPX-44) and the IMobS3 Laboratory of Excellence (ANR-10-LABX-16-01), by the European Union and the region Auvergne through the program L'Europe s'engage en Auvergne avec le fond européen de développement regional (FEDER).

REFERENCES

- Ait-Aider, O., Andreff, N., Lavest, J. M., and Martinet, P. (2006). Simultaneous object pose and velocity computation using a single view from a rolling shutter camera. In *Computer Vision—ECCV 2006*, pages 56–68. Springer.
- Ait-Aider, O., Bartoli, A., and Andreff, N. (2007). Kinematics from lines in a single rolling shutter image. In *Computer Vision and Pattern Recognition, 2007. CVPR'07. IEEE Conference on*, pages 1–6. IEEE.
- Ait-Aider, O. and Berry, F. (2009). Structure and kinematics triangulation with a rolling shutter stereo rig. In *Computer Vision, 2009 IEEE 12th International Conference on*, pages 1835–1840. IEEE.
- Anderson, S. and Barfoot, T. D. (2013). Towards relative continuous-time slam. In *Robotics and Automation (ICRA), 2013 IEEE International Conference on*, pages 1033–1040. IEEE.
- Baker, S., Bennett, E., Kang, S. B., and Szeliski, R. (2010). Removing rolling shutter wobble. In *Computer Vision and Pattern Recognition (CVPR), 2010 IEEE Conference on*, pages 2392–2399. IEEE.
- Bradley, D., Atcheson, B., Ihrke, I., and Heidrich, W. (2009). Synchronization and rolling shutter compensation for consumer video camera arrays. In *Computer Vision and Pattern Recognition Workshops*,

2009. *CVPR Workshops 2009. IEEE Computer Society Conference on*, pages 1–8. IEEE.
- Hartley, R. and Zisserman, A. (2003). *Multiple view geometry in computer vision*. Cambridge university press.
- Hedborg, J., Forssén, P.-E., Felsberg, M., and Ringaby, E. (2012). Rolling shutter bundle adjustment. In *Computer Vision and Pattern Recognition (CVPR), 2012 IEEE Conference on*, pages 1434–1441. IEEE.
- Hedborg, J., Ringaby, E., Forssén, P.-E., and Felsberg, M. (2011). Structure and motion estimation from rolling shutter video. In *Computer Vision Workshops (ICCV Workshops), 2011 IEEE International Conference on*, pages 17–23. IEEE.
- Horn, B. K. (1987). Closed-form solution of absolute orientation using unit quaternions. *JOSA A*, 4(4):629–642.
- Li, M., Kim, B. H., and Mourikis, A. I. (2013). Real-time motion tracking on a cellphone using inertial sensing and a rolling-shutter camera. In *Robotics and Automation (ICRA), 2013 IEEE International Conference on*, pages 4712–4719. IEEE.
- Liang, C.-K., Chang, L.-W., and Chen, H. H. (2008). Analysis and compensation of rolling shutter effect. *Image Processing, IEEE Transactions on*, 17(8):1323–1330.
- Magerand, L., Bartoli, A., Ait-Aider, O., and Pizarro, D. (2012). Global optimization of object pose and motion from a single rolling shutter image with automatic 2d-3d matching. In *Computer Vision–ECCV 2012*, pages 456–469. Springer.
- Meilland, M., Drummond, T., and Comport, A. I. (2013). A unified rolling shutter and motion blur model for 3d visual registration. In *The IEEE International Conference on Computer Vision (ICCV)*.
- Meingast, M., Geyer, C., and Sastry, S. (2005). Geometric models of rolling-shutter cameras. *arXiv preprint cs/0503076*.
- Mouragnon, E., Lhuillier, M., Dhome, M., Dekeyser, F., and Sayd, P. (2009). Generic and real-time structure from motion using local bundle adjustment. *Image and Vision Computing*, 27(8):1178–1193.
- Ringaby, E. and Forssén, P.-E. (2012). Efficient video rectification and stabilisation for cell-phones. *International journal of computer vision*, 96(3):335–352.
- Royer, E., Lhuillier, M., Dhome, M., and Lavest, J.-M. (2007). Monocular vision for mobile robot localization and autonomous navigation. *International Journal of Computer Vision*, 74(3):237–260.
- Saurer, O., Koser, K., Bouguet, J.-Y., and Pollefeys, M. (2013). Rolling shutter stereo. In *The IEEE International Conference on Computer Vision (ICCV)*.
- Tsai, R. Y. (1986). An efficient and accurate camera calibration technique for 3d machine vision. In *Proc. IEEE Conf. on Computer Vision and Pattern Recognition, 1986*.